

**ON THE ACCELERATION OF THE COUPLED-
INTEGRAL-EQUATIONS TECHNIQUE AND ITS
APPLICATION TO MULTISTUB E-PLANE
DISCONTINUITIES**

S. Amari and J. Bornemann

Department of Electrical and Computer Engineering
University of Victoria
Victoria, B.C., Canada

R. Vahldieck

Laboratory for Field Theory and Microwave Electronics
Swiss Federal Institute of Technology, ETH-Zentrum
8092 Zürich, Switzerland

Abstract—A technique to accelerate the numerical solution of scattering from multiple waveguide discontinuities by the Coupled-Integral-Equations Technique (CIET) is presented. The sums appearing in the numerical solution of the integral equations are computed at an initial frequency point and then used to accelerate the analysis at subsequent frequency points. Only few, typically 2 to 3, terms are needed to reach convergence for all structures investigated. Basis functions which include the edge conditions are used to guarantee numerical efficiency. A special routine to take advantage of the sparsity of the matrix relating the expansion coefficients to the incident excitation is also used. The method is applied to determine the scattering from rectangular waveguide E-plane discontinuities as well as multistub E-plane structures. Results from this work are compared to measurement and to those from the Mode-Matching Technique (MMT) to demonstrate its superiority.

1. INTRODUCTION

Waveguide discontinuities are important structures in modern waveguide implementations of filtering, matching, multiplexing, and polarizing devices. Accurate prediction of the frequency performance of these devices requires an efficient analysis of the effect of the discontinuities on incident fields as well as the interaction between the discontinuities.

Waveguide discontinuities and their interactions are commonly analyzed by the Mode-Matching Technique (MMT) where the scattering matrices of the individual discontinuities are determined separately and then cascaded to obtain the overall response, e.g., [1, 2]. Although the effect of the sharp metallic edges is taken into account in modified versions of the MMT to calculate the individual scattering matrices [3, 4], the interactions between the discontinuities is still determined by cascading the individual scattering matrices, thereby considerably limiting the effect of the edge conditions.

A systematic account of both the edge conditions as well as the interactions between the discontinuities is achievable through the Coupled-Integral-Equations Technique (CIET) [5]. Within this framework, the modes of the uniform sections are given a minor role in favor of the transverse fields at the discontinuities in terms of which the problem is reformulated. The interactions between the discontinuities are systematically accounted for regardless of their strength. The primary computational effort in this technique consists in computing inner products in the moment method solutions. These inner products involve infinite sums over the modes of the uniform sections of the waveguides.

The research reported in this paper constitutes a step towards developing techniques which allow the analysis of waveguiding structures with an arbitrarily large number of discontinuities within extremely short CPU times. With this ultimate goal in mind, we propose to further improve on the CIET by accelerating the convergence of the infinite sums which appear in computing inner products and taking advantage of the sparsity of the matrix relating the expansion coefficients of the electric field at the discontinuities to the incident excitation.

Although the problem of an E-plane step discontinuity is a classic problem in scattering of guided electromagnetic waves, it is revisited here to illustrate the salient features of the approach. The approach will be applied to multistub arrangements in subsequent sections.

2. ANALYSIS OF E-PLANE STEP DISCONTINUITIES

An E-plane step discontinuity is first considered to illustrate the essential features of the approach, especially the acceleration of the technique. The structure under consideration is depicted in figure 1. It consists of an E-plane step discontinuity at the junction of two rectangular waveguides of cross sections $a \times b_1$ and $a \times b_2$, respectively. All metallic walls are assumed lossless. We also assume that only the fundamental mode of the rectangular waveguide, TE_{10} , is incident from the larger waveguide with amplitude equal to unity at the angular frequency ω . Due to the symmetry of the structure, only TE_{to-x} modes are excited by the incident TE_{10} mode whose dependence on x , $\sin[\frac{\pi x}{a}]$, is suppressed from this discussion as it is common to all the excited modes.

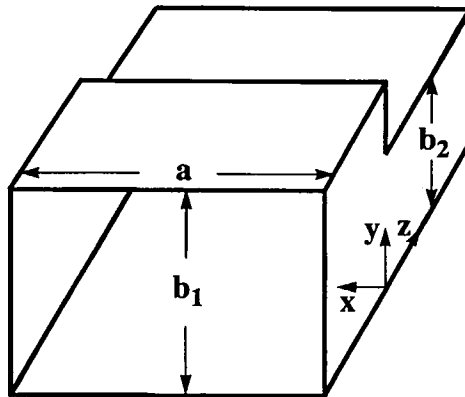


Figure 1. Geometry of an E-plane step discontinuity in a rectangular waveguide.

If we assume that the true distribution of the electric field at the discontinuity plane is denoted by $X(y)$ (apart from $\sin[\frac{\pi x}{a}]$), the following integral equation can be derived [6]

$$\sum_{m=0}^{\infty} Y_m^I \cos \left[\frac{m\pi y}{b_1} \right] \frac{2}{b_1(1 + \delta_{m0})} \int_0^{b_2} X(y') \cos \left[\frac{m\pi y'}{b_1} \right] dy' + \sum_{m=0}^{\infty} Y_m^{II} \cos \left[\frac{m\pi y}{b_2} \right] \frac{2}{b_2(1 + \delta_{m0})} \int_0^{b_2} X(y') \cos \left[\frac{m\pi y'}{b_2} \right] dy' = 2Y_0^I, \tag{1}$$

Here, $k_0 = \omega^2 \mu_0 \epsilon_0$, $k_{zm}^I = \sqrt{k_0^2 - (\frac{\pi}{a})^2 - (\frac{m\pi}{b_1})^2}$ and $Y_m^I(\omega) = \frac{k_0^2 - (\frac{\pi}{a})^2}{\omega \mu_0 k_{zm}^I}$ with similar expressions for the corresponding quantities in region II.

The notations \tilde{X}_m^I and \tilde{X}_m^{II} are introduced for convenience.

$$\tilde{X}_m^I = \frac{2}{b_1(1 + \delta_{m0})} \int_0^{b_2} X(y) \cos \left[\frac{m\pi y}{b_1} \right] dy \quad (2)$$

and

$$\tilde{X}_m^{II} = \frac{2}{b_2(1 + \delta_{m0})} \int_0^{b_2} X(y) \cos \left[\frac{m\pi y}{b_2} \right] dy \quad (3)$$

The solution of this integral equation has been extensively discussed in [6] and [7] mainly using the static approximation. Here we are not interested in its solution at a *single* frequency point, but rather over a range of frequency points. The first and straightforward approach consists in solving it repeatedly at each frequency point. An alternative and more efficient approach consists in solving the equation *once* and then use this solution to reduce the numerical effort at subsequent frequency points. The two alternatives are discussed next.

2.1 Direct Solution of Integral Equation

A direct numerical solution of the integral equation for the transverse electric field at the gap of the discontinuity by the moment method starts by expanding the unknown function in a series of basis functions [8]

$$X(y) = \sum_{r=1}^M c_r B_r(y). \quad (4)$$

The number of terms in the series is increased until convergence is reached. Using this expansion in the integral equation and applying Galerkin's method we obtain a set of linear equations in the expansion coefficients c_r

$$[A(\omega)][c] = [U(\omega)]. \quad (5)$$

The entries of the matrix $[A(\omega)]$ and the column vector $[U(\omega)]$ are given by

$$\begin{aligned}
 [A(\omega)]_{pq} = & \sum_{m=0}^{\infty} (1 + \delta_{m0}) \left\{ Y_m^I(\omega) \tilde{B}_p^I(m) \tilde{B}_q^I(m) \right. \\
 & \left. + \frac{b_2}{b_1} Y_m^{II}(\omega) \tilde{B}_p^{II}(m) \tilde{B}_q^{II}(m) \right\} \tag{6}
 \end{aligned}$$

and

$$[U(\omega)]_p = 4 \frac{b_2}{b_1} Y_0^I(\omega) \tilde{B}_p^{II}(0), \tag{7}$$

An important observation is necessary here. From the form of the matrix equation giving the vector $[c]$, i.e., equation (5), it is easily seen that the solution is not affected if *both* the matrix $[A]$ and the vector $[U]$ are multiplied (or divided) by the same scalar. In all what follows, all entries of the matrices $[A]$ and $[U]$ are divided by the term $k_0^2 - (\frac{\pi}{a})^2$ and multiplied by $\omega\mu_0$. This is systematically realized by taking the wave admittances to be $Y_m := \frac{1}{k_{zm}}$. Therefore and from here on, the wave admittances appearing in all matrix elements represent the quantities $\frac{1}{k_{zm}}$ and not the standard wave admittances.

A salient feature of the direct solution of the integral equation is the fact that the sums in $[A(\omega)]_{pq}$ are computed *ab initio* for each new frequency point. From the expressions of the wave admittances $Y_m^I(\omega)$ and $Y_m^{II}(\omega)$, it can be easily seen that they decrease as $\frac{1}{m}$ for large values of m ; a relatively large number of terms may be needed to reach convergence. An alternative solution which extracts more frequency-independent features from the solution at the first frequency point, and stores it for usage at other frequency points, will certainly be more efficient. Such an alternative is presented in the next section.

2.2 Acceleration of Numerical Solution

Let us assume that the entries of the matrix $[A(\omega)]$ have been computed at a given frequency point ω_0 , i.e., $[A(\omega_0)]$ is known. At another frequency point ω_1 , a generic element of the matrix $[A(\omega_1)]$ can be written as

$$\begin{aligned}
 [A(\omega_1)]_{pq} = & [A(\omega_0)]_{pq} \\
 & + \sum_{m=0}^{\infty} (1 + \delta_{m0}) \left\{ [Y_m^I(\omega_1) - Y_m^I(\omega_0)] \tilde{B}_p^I(m) \tilde{B}_q^I(m) \right.
 \end{aligned}$$

$$+ \frac{b_2}{b_1} \left[Y_m^{II}(\omega_1) - Y_m^{II}(\omega_0) \right] \tilde{B}_p^{II}(m) \tilde{B}_q^{II}(m) \left. \vphantom{\frac{b_2}{b_1}} \right\} \quad (8)$$

For large values of m , the terms appearing in the sums in this last equation decrease as $\frac{1}{m^3}$ instead of $\frac{1}{m}$; fewer terms are needed to reach convergence. As the numerical results will show, only 2 or 3 terms are needed in the residual sums for the structures investigated here. It is again important to recall that the “wave admittances” appearing in these equations are taken as $Y_m = \frac{1}{k_{zm}}$; otherwise the differences in the equations above will not have the stated asymptotic form.

2.3 Basis Functions

To guarantee numerical efficiency, the basis functions used in the moment method solution of the integral equation should contain the singular nature of the transverse electric field at the metallic wedge of the discontinuity as well as other pivotal *a priori* information about the solution. At a 90-degree metallic wedge, the components of the electric field, which are normal to the axis of the wedge, become singular as $r^{-1/3}$ as $r \rightarrow 0$ where r is the radial distance from the wedge [9]. Furthermore, at the flat metallic wall of the waveguide, the normal component of the electric field approaches a constant. The following set of basis functions satisfies these two local conditions.

$$B_r(y) = \frac{\cos \left[\frac{r\pi y}{b_2} \right]}{\left[1 - \left(\frac{y}{b_2} \right)^2 \right]^{1/3}}, \quad r = 0, 1, \dots \quad (9)$$

The spectra of these basis functions in the two regions can be expressed in terms of Bessel functions of order 1/6 [10]

$$\tilde{B}_r^I(m) = \frac{b_1}{2b_2} \Gamma(1/2)\Gamma(2/3) \left\{ \frac{J_{1/6} \left[\left| r - m \frac{b_1}{b_2} \right| \pi \right]}{\left[\left| r - m \frac{b_1}{b_2} \right| \frac{\pi}{2} \right]^{1/6}} + \frac{J_{1/6} \left[\left| r + m \frac{b_1}{b_2} \right| \pi \right]}{\left[\left| r + m \frac{b_1}{b_2} \right| \frac{\pi}{2} \right]^{1/6}} \right\} \quad (10)$$

and

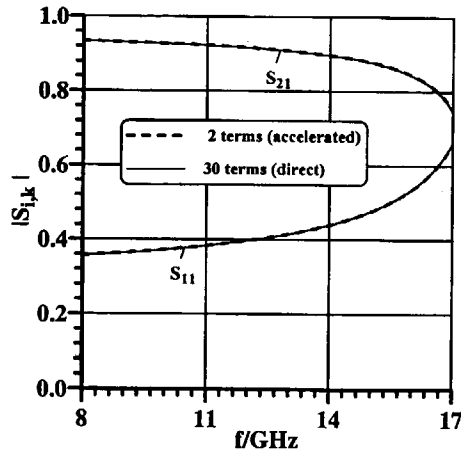


Figure 2. Reflection and transmission coefficient of the discontinuity in figure 1: Direct CIET with 30 terms (dashed line), accelerated CIET with 2 terms (solid line). Two basis functions are used. Dimensions: $a = 19.05$ mm, $b_1 = 9.525$ mm, $b_2 = 4.52$ mm.

$$\bar{B}_r^{II}(m) = \frac{1}{2}\Gamma(1/2)\Gamma(2/3) \left\{ \frac{J_{1/6}[|r - m|\pi]}{[|r - m|\frac{\pi}{2}]^{1/6}} + \frac{J_{1/6}[|r + m|\pi]}{[|r + m|\frac{\pi}{2}]^{1/6}} \right\} \quad (11)$$

From the asymptotic forms of the Bessel functions, it follows that these spectra decrease as $m^{-2/3}$ for large values of m .

In order to demonstrate the influence of the acceleration procedure, the present form of the Coupled-Integral-Equations Technique (CIET) is applied to the E-plane discontinuity of figure 1.

Figure 2 shows the reflection and transmission coefficients as a function of frequency when 30 terms are retained in the sums of the direct CIET (solid line) and when only two terms are retained in the accelerated form of the CIET. Two basis functions were used in both cases. More basis functions were used and resulted in no noticeable difference. A CPU time comparison shows that for 200 frequency points, the accelerated version is about twice as fast as the direct CIET.

The convergence of the solution as a function of the number of terms in the sums in equation (8) is shown in figure 3. The differences between the results with only two terms and those with 5 terms are

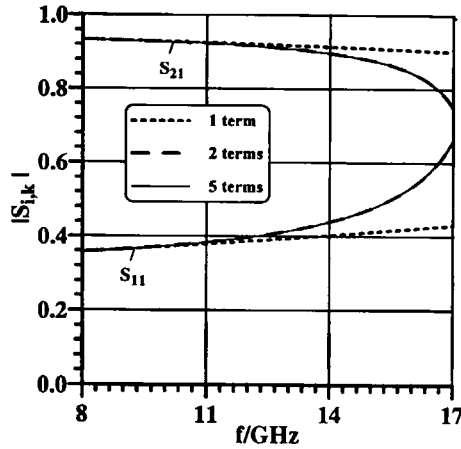


Figure 3. Convergence of the accelerated CIET as a function of the number of terms in the residual sums: 1 term (dotted line), 2 terms (dashed line), 5 terms (solid line). Two basis functions are used. Dimensions as in Fig. 2.

minor; they agree within plotting accuracy. When only one term is retained in the residual sums, both the reflection and the transmission coefficients are accurately predicted for frequencies lower than 10 GHz.

2.4 Analysis of an E-Plane Stub

The previous section presented a detailed discussion of the technique we use to accelerate the convergence of the numerical solution of the original frequency dependent scattering problem. In this section, we apply the technique to an E-plane stub as shown in the inset of figure 4. We again assume that the fundamental mode of the rectangular waveguide, TE_{10} , is incident on the stub with amplitude equal to unity.

This structure was analyzed in [3] using a combination of the generalized scattering matrix and an analysis similar to what was presented in the previous section.

Because of the symmetry of the structure, the integral equations for the transverse electric field at the two discontinuities are also symmetric. The steps in the derivation are similar to those of the multiple H-plane discontinuities [5], and the reader is referred to [5] for the computation of the three- and seven-stub configurations of Section III.

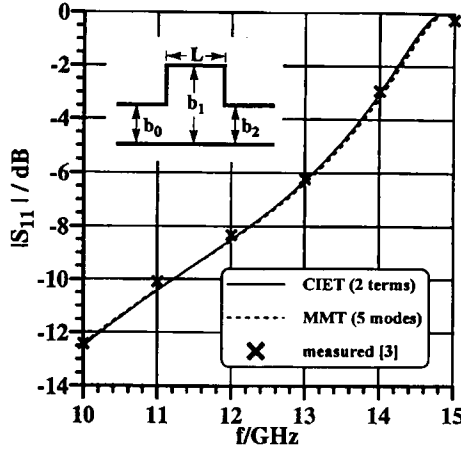


Figure 4. Reflection coefficient of a single E-plane stub as a function of frequency: Accelerated CIET with 2 basis functions (solid line), mode-matching technique (MMT) with 5 modes (dashed line), measurement (x) from [3]. Dimensions: $a = 19.05$ mm, $b_0 = b_2 = 9.525$ mm, $b_1 = 12.98$ mm, $L = 7.68$ mm.

In order to demonstrate the underlying principle in multistub analyses, we present the two coupled integral equations for the electric field $X_1(y)$ and $X_2(y)$ at the two discontinuities of a single stub:

$$\begin{aligned}
 & - \sum_{m=0}^{\infty} Y_m^{II} \left[\frac{\tilde{X}_2^{II}(m)}{\sin[k_m^{II}L]} - \frac{\tilde{X}_1^{II}(m)}{\tan(k_m^{II}L)} \right] \cos \left[m\pi \frac{y}{b_1} \right] \\
 & + j \sum_{m=0}^{\infty} Y_m^I \tilde{X}_1^I(m) \cos \left[m\pi \frac{y}{b} \right] = 2jY_0^I \quad (12)
 \end{aligned}$$

and

$$\begin{aligned}
 & - \sum_{m=0}^{\infty} Y_m^{II} \left[\frac{\tilde{X}_1^{II}(m)}{\sin[k_m^{II}L]} - \frac{\tilde{X}_2^{II}(m)}{\tan(k_m^{II}L)} \right] \cos \left[m\pi \frac{y}{b_1} \right] \\
 & + j \sum_{m=0}^{\infty} Y_m^I \tilde{X}_2^I(m) \cos \left[m\pi \frac{y}{b} \right] = 0. \quad (13)
 \end{aligned}$$

The transformed functions $\tilde{X}^I(m)$ and $X^{II}(m)$ in these two equations are given by

$$\tilde{X}^I(m) = \frac{2}{b} \frac{1}{1 + \delta_{m0}} \int_0^b X(y) \cos \left[m\pi \frac{y}{b} \right] dy \quad (14)$$

and

$$\tilde{X}^{II}(m) = \frac{2}{b_1} \frac{1}{1 + \delta_{m0}} \int_0^b X(y) \cos \left[m\pi \frac{y}{b_1} \right] dy. \quad (15)$$

To solve these two coupled integral equations, we expand the two functions in series of basis functions. Since the two discontinuities have essentially the same geometry, we use the same sets of basis functions to expand both $X_1(y)$ and $X_2(y)$.

$$X_1(y) = \sum_r d_r B_r(y) \quad (16)$$

and

$$X_2(y) = \sum_s e_s B_s(y) \quad (17)$$

Applying Galerkin's method, we obtain two sets of linear equations in the expansion coefficients d and e

$$\begin{aligned} [A(\omega)][d] + [B(\omega)][e] &= [C(\omega)] \\ [B(\omega)][d] + [A(\omega)][e] &= 0 \end{aligned} \quad (18)$$

The entries of the matrices in this equation at a frequency ω_1 are given in terms of those at ω_0 by

$$\begin{aligned} [A(\omega_1)]_{pq} &= [A(\omega_0)]_{pq} + \sum_{m=0}^{\infty} (1 + \delta_{m0}) \\ &\cdot \left\{ \left[\frac{Y_m^{II}(\omega_1)}{\tan[k_m^{II}(\omega_1)L]} - \frac{Y_m^{II}(\omega_0)}{\tan[k_m^{II}(\omega_0)L]} \right] \tilde{B}_p^{II}(m) \tilde{B}_q^{II}(m) \right. \\ &\left. + j \frac{b}{b_1} [Y_m^I(\omega_1) - Y_m^I(\omega_0)] \tilde{B}_p^I(m) \tilde{B}_q^I(m) \right\}, \end{aligned} \quad (19)$$

$$\begin{aligned} [B(\omega_1)]_{pq} &= [B(\omega_0)]_{pq} - \sum_{m=0}^{\infty} \left[\frac{Y_m^{II}(\omega_1)}{\sin[k_m^{II}(\omega_1)L]} - \frac{Y_m^{II}(\omega_0)}{\sin[k_m^{II}(\omega_0)L]} \right] \\ &\cdot \tilde{B}_p^{II}(m) \tilde{B}_q^{II}(m) (1 + \delta_{m0}), \end{aligned} \quad (20)$$

and

$$[C]_p = 4jY_0^I(\omega_1)\bar{B}_p^I(0)\frac{b}{b_1}. \quad (21)$$

For large values of m , the wave admittances become imaginary since they correspond to evanescent modes. In this limit, $\tan(k_{zm}L) \rightarrow j \tanh(|k_{zm}|L) \rightarrow 1$ and $\sin(k_{zm}L) \rightarrow j \sinh(|k_{zm}|L) \rightarrow e^{|k_{zm}|L}$. The terms in the sums in the above equations have the same asymptotic form as in the case of a single discontinuity although this asymptotic form may be reached at larger values of m , especially for small values of L . Furthermore, "connecting" elements involve terms of the form $\frac{Y_m}{\sin(k_{zm}L)}$ and decrease exponentially when m is large. Consequently, only very few terms are needed for these matrix elements.

3. RESULTS

The basis functions of the last section are used to determine the return and insertion loss of the stub analyzed in reference [3]. Figure 4 shows the reflection coefficient of this stub as a function of frequency. The solid line are results obtained from the present approach using 2 basis functions. The dashed line are the results from the standard Mode-Matching Technique (MMT) using five modes but no edge conditions. (Note that the number of modes in MMT is increased within the stubs according to the height ratios.) These are identical to those presented in [3] and [11] within the readability of the quoted results. The agreement between the calculations and the measured values from reference [3] is excellent. Note, however, that the results obtained from the CIET move slightly closer to the experimental values.

Figure 5 shows the reflection coefficient in dB of a three-stub structure as investigated in [3]. Three basis functions are used at each discontinuity within the accelerated CIET. Also shown are the results obtained from MMT using 5 modes (dotted line) and 15 modes (dashed line). The agreement between the simulated results and the measured values of [3] is excellent.

A comparison between the results from the present work and those obtained from the MMT with the proper edged conditions [3], or the multimode model presented in [11], shows that the location of the resonance peak occurs at a lower frequency in our results, i.e., closer to the experimental location. Both methods presented in references [3] and [11] predict this peak at 11 GHz. Results from the CIET indicate the resonance to be at 10.90 GHz. The measured location

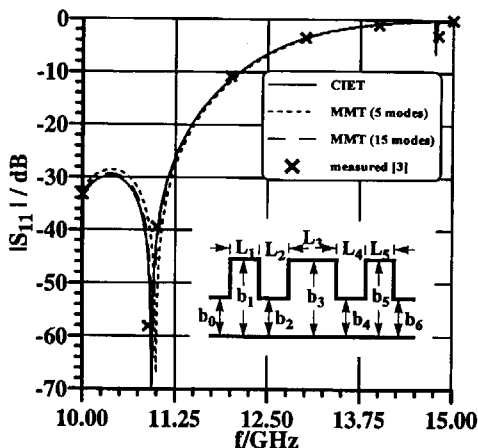


Figure 5. Reflection coefficient of a three-stub structure as a function of frequency: Accelerated CIET with 3 basis functions (solid line), MMT with 5 modes (dotted line) and 15 modes (dashed line), measurement (\times) from [3]. Dimensions: $a = 19.05$ mm, $b_0 = b_2 = b_4 = b_6 = 9.525$ mm, $b_1 = b_3 = b_5 = 12.98$ mm, $L_1 = L_5 = 4.29$ mm, $L_2 = L_4 = 4.61$ mm, $L_3 = 7.68$ mm.

is, within the readability of the results from [11], 10.88 GHz. The second resonance, which occurs around 14.8 GHz, is also present in the CIET results and in the multimode model [11]. It is also present in the standard MMT, but only when a large enough number of modes is used, i.e., when convergence is reached. Note that the results of the simulations presented in [11], which predict a main resonance at 11 GHz, are identical to those obtained from the standard MMT with 5 modes. If the number of modes is increased, the location of the resonance moves towards lower frequencies and converges to 10.92 GHz. The same location is obtained from the CIET with only three basis function at each of the six discontinuities.

Convergence tests performed for the transmission coefficient lead to similar conclusions and are not shown here. The results obtained from cascading the scattering matrices, with and without the edge conditions, and with the same number of accessible modes, appear to be identical, and less accurate than those of the CIET with the same number of basis functions, despite the fact that the inclusion of the edge condition considerably reduces the CPU time required to compute the scattering matrices.

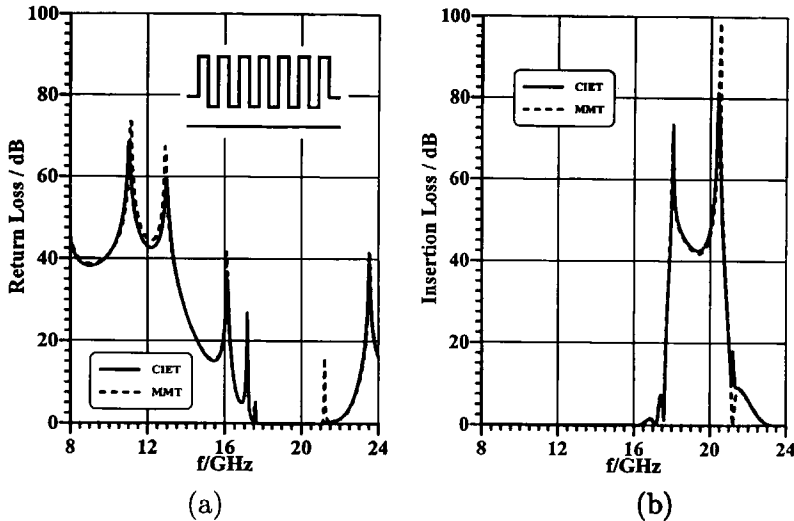


Figure 6. Computed performance of a seven-stub band-pass/band-reject filter: Accelerated CIET with 18 terms and 4 basis functions (solid line), MMT with 9 modes at input and 18 modes within stubs. a) Return loss, b) Insertion loss.

Figures 6 show the computed performance of a seven-stub band-pass/band-reject filter as used in diplexing applications, e.g., [12]. In order to not only avoid the issue of determining the number of accessible modes and cascading the scattering matrices, in which the modes of the uniform sections play an unduly crucial role, but still to accurately account for the strong interactions between the different discontinuities, we formulate the problem in *one step* and include the proper edge conditions at each of the discontinuities.

The return loss and insertion loss of the filter using the accelerated CIET and the MMT are depicted in figure 6a and 6b, respectively. The agreement between the results of the two simulations is excellent. In order to obtain a fair comparison with respect to the CPU times involved, a conversion analysis was first performed with the MMT. This resulted in nine modes at the input and, since the stubs are about twice as high as the input guide, 18 modes in the stub sections. The corresponding number of terms for the same field resolution in the CIET is 18. For 320 frequency samples and using 4 basis functions and 3 terms in the acceleration process, the accelerated CIET is 2.1 times as fast as the direct CIET, and 28 times as fast as the MMT.

More modes in the MMT as well as more basis functions in the accelerated CIET yield negligible changes in both the return and insertion losses of figures 6a and b. An increased advantage of the accelerated CIET versus the MMT is obtained for structures requiring more modes (terms). As an example, the same seven-stub band-pass/band-reject filter was recalculated with 30 terms (30 modes in the subsections, 15 at input), while all other parameters remained identical. In this case, the accelerated CIET turned out to be 2.8 times as fast as the direct CIET, but 100 times as fast as the MMT.

4. CONCLUSIONS

A technique to accelerate the numerical solution of scattering from multiple waveguide discontinuities by the Coupled-Integral-Equation Technique (CIET) is presented. Numerical results show that only a few terms contribute to the residual sums in the inner products. A substantial reduction in CPU time (compared to MMT) is achieved, first, when multiple discontinuities are analyzed in a single step, where all edge conditions are included simultaneously, and the sparsity of the matrix $A(\omega)$ is taken into account (direct CIET); and second, when the computation of the entries of that matrix is accelerated by attributing much of the computational effort to a single frequency, i.e., $A(\omega_0)$, (accelerated CIET). The speed and accuracy of this technique makes it possible to analyze structures with a large number of discontinuities. Excellent agreement between the results from the present approach, measurements and the MMT is documented.

REFERENCES

1. Itoh, T., ed., *Numerical Techniques for Microwave and Millimeter-Wave Passive Structures*, John Wiley & Sons, New York 1989.
2. Uher, J., J. Bornemann, and U. Rosenberg, *Waveguide Components for Antenna Feed Systems: Theory and CAD*, Artech House, Boston, 1993.
3. Rozzi, T. and M. Mongiardo, "E-plane steps in rectangular waveguides," *IEEE Trans. Microwave Theory Tech.*, Vol. 30, 1279–1288, Aug. 1991.
4. Sorrentino, R., M. Mongiardo, F. Alessandri, and G. Schiavon, "An investigation of the numerical properties of the Mode-Matching Technique," *Int. J. Numerical Modelling*, Vol. 4, 19–43, March 1991.

5. Amari, S., J. Bornemann, and R. Vahldieck, "Accurate analysis of scattering from multiple waveguide discontinuities using the coupled-integral-equations technique," *J. Electromagnetic Waves & Applications*, Vol. 10, 1623–1644, Dec. 1996.
6. Schwinger, J. and D. S. Saxon, *Discontinuities in Waveguides*, Gordon and Breach, New York, 1968.
7. Lewin, L., *Theory of Waveguides*, Newnes-Butterworths, London, 1975.
8. Harrington, R. F., *Field Computation by Moment Methods*, Krieger, Malabar, FL. 1987.
9. Collin, R. E., *Field Theory of Guided Waves*, IEEE Press, New York, 1991.
10. Gradshteyn, I. S. and I. M. Ryznik, *Tables of Integrals, Series, and Products*, Fifth Edition, Academic Press, New York, 1994.
11. Weisshaar, A., M. Mongiardo, A. Tripathi, and V. K. Tripathi, "CAD-oriented full-wave equivalent circuit models for waveguide components and circuits," *IEEE Trans. Microwave Theory Tech.*, Vol. 44, 2564–2570, Dec. 1996.
12. Bornemann, J., J. Uher, and K. Patel, "Efficient full-wave CAD of waveguide diplexers," in *Proc. ANTEM'96 Symp. Antenna Tech. and Applied Electromag.*, Montreal, Canada, Aug. 1996.

Smain Amari received his DES in physics and electronics from Constantine University (Algeria) in 1985, the M.S. degree in electrical engineering in 1989 and the Ph.D. degree in physics in 1994 both from Washington University in St. Louis. He is interested in numerical methods in electromagnetics, numerical analysis, applied mathematics, applied physics and application of quantum field theory in quantum many-particle systems. Since 1994, he has been with the Department of Electrical and Computer Engineering at the University of Victoria, Canada.

Jens Bornemann received the Dipl.-Ing. and the Dr.-Ing. degrees, both in electrical engineering, from the University of Bremen, Germany, in 1980 and 1984, respectively. He is currently a Professor in the ECE Department, University of Victoria, B.C., Canada. His research activities focus on microwave components design, and electromagnetic field theory in circuits and antennas. Dr. Bornemann is a senior member of IEEE and serves on the editorial board of *IEEE Trans. MTT* and *Int. J. of Numerical Modelling*. He has (co)authored more than 140 technical papers and a book on *Waveguide Components for Antenna Feed Systems—Theory and CAD*, Artech House, 1993.

Rüdiger Vahldieck received the Dipl.-Ing. and the Dr.-Ing. degrees in electrical engineering from the University of Bremen, Germany, in 1980 and 1983, respectively. From 1984 to 1986, he was a Research Associate at the University of Ottawa, Canada. In 1986 he joined the ECE Department at the University of Victoria, B.C., Canada, where he became a Full-Professor in 1991. During Fall and Spring 1992–1993 he was a visiting scientist at the Ferdinand-Braun-Institute für Hochfrequenztechnik in Berlin, Germany. Since October 1996 he has been the Chair of Field Theory at the Laboratory for Electromagnetic Fields and Microwave Electronics at the Swiss Federal Institute of Technology in Zürich, Switzerland. His research interests include numerical methods to model electromagnetic fields for computer-aided design of microwave, millimeter-wave and opto-electronic integrated circuits. Dr. Vahldieck, together with three coauthors, received the outstanding publication award of the Institution of Electronic and Radio Engineers in 1983. He is on the editorial board of the *IEEE Trans. MTT* and serves on the Technical Program Committee of the *IEEE Int. Microwave Symposium*. He has published more than 150 technical papers.